PHILOSOPHICAL TRANSACTIONS OF THE ROYAL SOCIETY A MATHEMATICAL, PHYSICAL & ENGINEERING SCIENCES

An Area on the Crest of the Carlsberg Ridge: Petrology and Magnetic Survey

J. R. Cann and F. J. Vine

Phil. Trans. R. Soc. Lond. A 1966 **259**, 198-217
doi: 10.1098/rsta.1966.0007

An area on the crest of the Carlsberg Ridge: petrology and magnetic survey

By J. R. Cann

Department of Mineralogy and Petrology, University of Cambridge

and F. J. Vine*

Department of Geodesy and Geophysics, University of Cambridge

[Plates 2 and 3]

Rocks collected in the vicinity of a transcurrent fault cutting the crest of the Ridge have been affected by brecciation and, in some cases, metamorphism and hydrothermal action. These processes have led to the formation of spilites from crystalline basalts, and ultramafic rocks from basalt glasses. Further hydrothermal action has taken the form of replacement of some ultramafic rocks by quartz, ending in a nearly pure quartzite. The mineralogy is characteristic of greenschist facies metamorphism.

Fresh basalts were collected from a nearby hill, which seems to be a recent volcano post-dating the faulting and metamorphism.

The magnetic survey reveals a marked parallelism between the anomalies and the trend of the ridge, regardless of bathymetry. Computations confirm that uniform magnetization of the material represented by the bathymetry can in no way simulate the observed anomalies. Application of a vector fitting technique suggests that the remanent magnetization of this material is often reversed and from this a very crude and simple model is developed to account for the observed anomalies. The model is consistent with an ocean floor spreading hypothesis and periodic reversals in the earth's magnetic field. If substantiated it would have important implications in deducing the history of the ocean basins. Above all it provides a plausible explanation to account for the magnetic gradients and amplitudes observed over ridges without implying improbable magnetic contrasts, structures, or changes in petrology.

Introduction

In November 1962, H.M.S. *Owen* made a detailed bathymetric, magnetic and gravity survey of an area on the crest of the Carlsberg Ridge (figure 1). The survey, centred on 5° 20′ N, 61° 50′ E, covers an area of 51 × 39 mi., its longer side being orientated N 40° E, that is, at right angles to the trend of the Ridge as deduced from earlier crossings. The average spacing of tracks parallel to the longer side of the survey area is 1 mi., and these tracks, together with crosstracks, produced virtually complete records from approximately 2000 mi. of continuous profiling. The resulting bathymetric chart for the area is presented in figure 2. In September 1963 R.R.S. *Discovery* returned to the area to carry out station work which included underwater photography and dredging.

A preliminary interpretation of the results (Matthews, Vine & Cann 1965) suggests that the area is traversed by a minor fault with a dextral strike slip of approximately 10 mi. The fault, indicated by the solid line in figure 2, has a pronounced trough associated with it and in the fault zone the characteristic magnetic relief of the crest of the ridge is expunged, presumably owing to brecciation and disorientation of the underlying rock.

* Present address: Department of Geology, Princeton University.

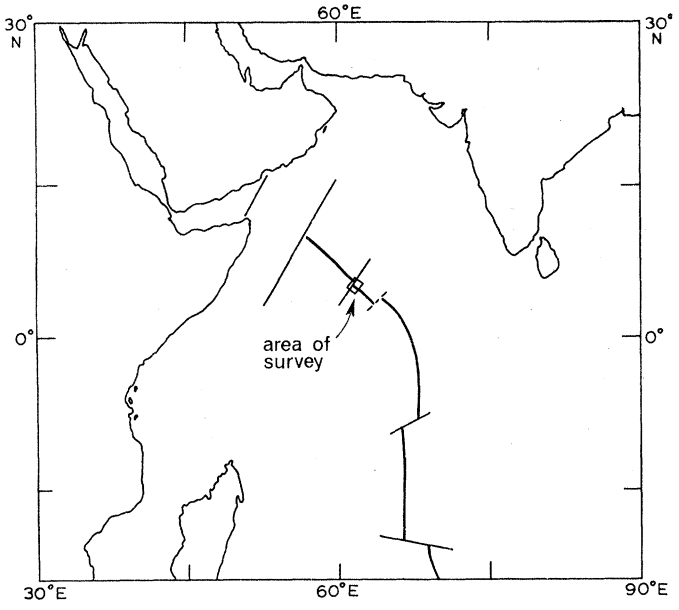

FIGURE 1. Map of the Arabian Sea showing the position of the survey area, the trend of the crest of the Ridge, and possible transcurrent faults associated with it.

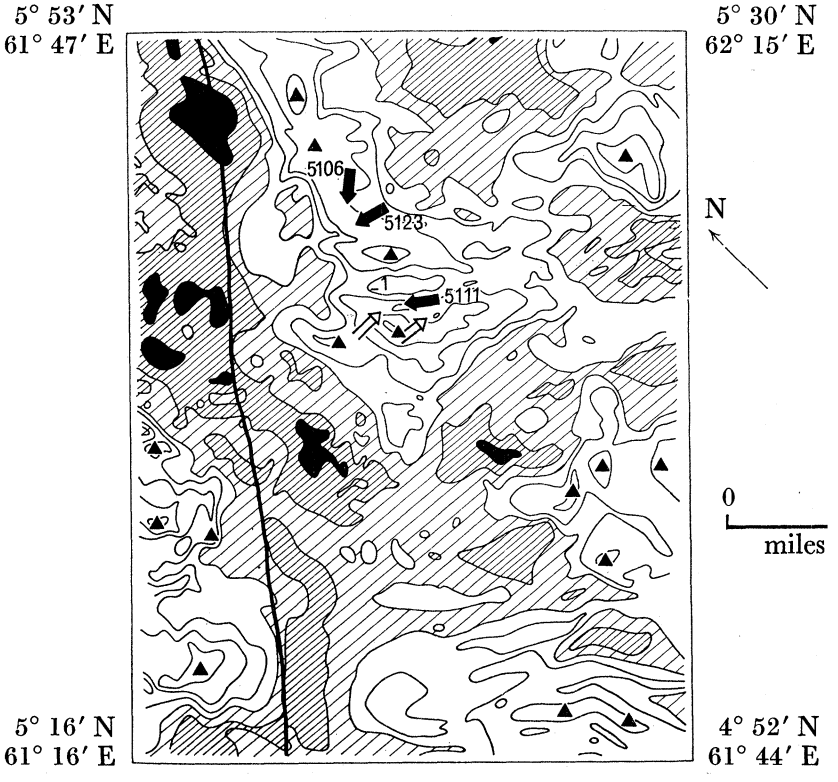

FIGURE 2. Bathymetry over the area of 51 × 39 mi. The contour interval is 200 fm. Depths greater than 1700 fm are shaded, depths greater than 2100 fm are solid black. Peaks shallower than 1300 fm are marked by solid triangles. The shading lines run east–west. The heavy line is the presumed fault. Three solid arrows mark the localities from which the dredge hauls were obtained; from north to south (top to bottom) they are Discovery Stations 5106, 5123 and 5111. The open arrows indicate underwater camera stations.

The particulars accompanying this figure, namely the coordinates of the corners of the survey area, the north pointing arrow and the scale, apply also to figures 4, 5, 7, 8, 9, 10 and 11.

Petrology

Successful dredge hauls were made at three stations in the area, 5106, 5111 and 5123, the positions of which are shown on figure 2.

(*a*) *Station* 5111

Station 5111 is on the flanks of the central elongate seamount. Underwater photographs taken by Dr A. S. Laughton at two stations nearby on the same hill (5113, 5121, marked on the bathymetric chart figure 2), showed fine outcrops of pillow lavas. The pillows are almost completely free of manganese encrustation and display glassy surfaces cut by closely spaced cooling cracks now filled with ooze. The haul from the dredge station contained one nearly complete pillow and several fragments of pillows associated with a glassy crust typical of those seen in the photographs.

Table 1. Analyses and norms of fresh basalts dredged from station 5111

	1 5111·2	2 5111·5		1A 5111·2	2A 5111·5
SiO_2	48·88	48·96	or	0·95	1·60
Al_2O_3	16·31	16·17	ab	24·96	24·79
Fe_2O_3	2·22	2·49	an	30·79	30·17
FeO	8·12	7·71	ol fo	7·41	6·20
MnO	0·20	0·17	ol fa	4·25	3·34
MgO	8·42	8·15	hy en	4·75	5·58
CaO	10·76	10·67	hy fs	2·47	2·73
Na_2O	2·95	2·93	di wo	9·11	9·31
K_2O	0·16	0·27	di en	5·64	5·87
TiO_2	1·54	1·51	di fs	2·93	2·87
P_2O_5	0·12	0·07	mt	3·22	3·61
H_2O+	0·61	0·62	il	2·92	2·87
H_2O-	0·19	0·31	ap	0·28	0·17
	100·48	100·03		99·69	99·11
			water	0·80	0·93
				100·49	100·04

Thin sections show that the rocks are microporphyritic olivine basalts typical of specimens dredged from elsewhere in the oceans (Muir & Tilley 1964; Nicholls, Nalwalk & Hays 1964; Engel & Engel 1963, 1964*a*, *b*, for example). In none of the specimens does olivine show a reaction relationship; olivine crystals of all sizes are found in considerable abundance even in the finest groundmass, and the rocks cannot thus be considered typical tholeiites. In one or two of the specimens the pyroxene has a lilac-brown colour suggesting alkaline rather than tholeiitic affinities.

Chemical analysis of two specimens (table 1) shows that these rocks are closely comparable in composition with many of the other analysed fresh basalts from the deep ocean. In their ratio of normative olivine to normative hypersthene they are close to that of specimen 4519.25 of Muir & Tilley (1964) which is best described as transitional between alkali and tholeiitic types on the basis of pyroxene composition as well as petrography and the same description is probably best used for these basalts too. The widespread occurrence of lavas on the deep sea floor which, though ranging from true tholeiites to true alkali basalts, are very closely comparable in composition has been remarked by Engel & Engel (1964*b*), although they consider all of the rocks to be tholeiites, and these specimens

serve further to extend the geographical range of this lava type.* Clearly magma of very much the same character has been erupted on the ocean floor at very widely separated places in at least the recent past. This composition is very different from that of the basalts of most oceanic islands which thus appear to be anomalies of the ocean bed rather than portions of it that happen to have risen above the sea. However, the postulate of Engel & Engel (1964*b*) that only magma of the ocean floor composition can be generated in the mantle and that the common alkali basalts and their derivatives of the oceanic islands are fractional crystallization products of this magma seems unnecessary. An equally possible hypothesis would be that the presence of an oceanic island or seamount of rather larger size than usual would modify the *P–T* conditions in the rocks beneath sufficiently to allow melting of the mantle at, for example, a greater depth than elsewhere beneath the sea floor, with the consequent production of alkali basalt magma. Such a hypothesis would have the merit of not contradicting the experimental evidence of Yoder & Tilley (1962) and Davis & England (1964), and the geophysical evidence of earthquake focus depth from Japan, while still being consistent with the field evidence from the oceans.

(*b*) *Station* 5106

Most of the rocks from this haul and from haul 5123, which were made close together on the line of hills flanking the fault trough, are of metamorphic origin.

Haul 5106 contained twenty-one generally small fragments of rock, nearly all of which have a brecciated or veined appearance in hand specimen. These were divided on the basis of thin section examination into four groups, three fresh basalts and basalt breccias, six spilites, three specimens of ultramafic mineralogy and nine rocks forming a series that shows the replacement of an ultramafic breccia by quartz.

(i) *Fresh basalt breccias*

These rocks are essentially composed of fragments of fresh basalt and basalt glass in a matrix of finely comminuted pieces of the same material. The glass fragments are often somewhat palagonitized, but fresh pale yellow isotropic glass is not rare. Most of the basalt fragments are completely fresh, but in some, which often lie next to fresh fragments, the initial stages of spilitization may be seen. Olivine microphenocrysts are replaced by chlorite, and vesicles, originally empty, become filled with chlorite and occasional quartz grains. The fresh fragments are petrographically and chemically very similar to the basalts from haul 5111 (although the analysed specimen (table 2, no. 1) is somewhat more tholeiitic), and belong to the same widespread magma type.

(ii) *Spilites*

The spilites have a texture very similar to that of the fresh basalts (figure 12, plate 2). Long skeletal needle-like plagioclase microphenocrysts are common, but instead of being composed of basic plagioclase, their composition is close to albite and they are cut by

* The basalts analysed by Wiseman (1937) from the Carlsberg Ridge at $1\frac{1}{2}^\circ$ S, although considered by Engel & Engel to be of this magma type, appear to be of rocks slightly or more completely spilitized, as will be shown later in this paper. Although their original compositions were probably close to those reported here, their present high Na_2O and H_2O+ and low CaO compared with other analyses of basalts from the deep ocean are the result of the spilitization.

PHILOSOPHICAL TRANSACTIONS OF THE ROYAL SOCIETY A MATHEMATICAL, PHYSICAL & ENGINEERING SCIENCES

minute veins and stringers of chlorite. Pseudomorphs after olivine microphenocrysts may be recognized by their characteristic shapes: they are now composed of flaky-aggregates of green chlorite. Vesicles have been filled with chlorite associated with occasional rounded quartz grains. In the ground mass, set in a base of green chlorite, are granular bunches of fine-grained augite, needles of albite and aggregates of very fine-grained sphene. Thin blades of actinolite and grains of epidote are also sometimes present. Fissure veins which cut the spilites are filled with quartz, chlorite, epidote, talc and sphene in various combinations, sometimes as relatively large crystals (up to 2 mm across).

The mineralogy is that usual for spilites. The chlorite is pale green and flaky, except in some veins where single crystals may be developed. A powder photograph gave $d_{(001)} = 14{\cdot}21$ Å and $d_{(010)} = 9{\cdot}26$ Å, the refractive index was $1{\cdot}600 \pm 0{\cdot}002$ (the birefringence being very low) and electron probe measurements indicated an iron content of about 17·3% calculated as FeO. These results indicate a composition near a magnesian pycnochlorite, following the classification of Hey (1954) (about $Mg_{6{\cdot}5}Fe^{II}_{3{\cdot}5}Al_4Si_6O_{20}(OH)_{16}$).

The felspar, with $\alpha = 1{\cdot}528 \pm 0{\cdot}002$, must be very close in composition to pure albite. The very fine-grained pyroxene, although it could not be separated for further investigation, appeared from its $2V$ to be a Ca-rich augite.

The birefringence of the epidote in the fissure veins varied from 0·046 to 0·050 for the common nearly colourless variety to 0·067 for a highly coloured and highly pleochroic epidote in one vein. Electron probe measurements showed that the common variety ranged in composition from $Cz_{81}Ps_{19}$ to $Cz_{74}Ps_{26}$, and the highly coloured variety from $Cz_{70}Ps_{30}$ to $Cz_{62}Ps_{38}$. Mn was always less than 0·3%.

Four chemical analyses were made to illustrate the change from fresh basalt to spilite. These may be seen in table 2. No. 1 is an analysis of a fresh basalt fragment from a basalt breccia, no. 2 of a basalt fragment in which the olivine phenocrysts are replaced and the vesicles filled, no. 3 of an incompletely spilitized dolerite containing relicts of Ca-rich plagioclase as islands in the crystals of albite, and no. 4 of a true spilite.

The broad picture of the chemical changes occurring can easily be seen: CaO and K_2O decrease sharply and Na_2O and H_2O+ increase just as markedly. Table 3 shows the same analyses calculated on the basis of grams of oxide in 100 ml. rock, so that comparison can be made on the assumption of constant volume changes, an assumption that cannot be far from the truth judging by the preservation of basaltic texture in the spilites. Making this assumption, 10·6 g of CaO and 0·7 g of K_2O must be removed from, and 5·7 g of Na_2O and 6·8 g of H_2O must be added to each 100 ml. of the fresh basalt to give the spilite. The only other change which appears significant is the decrease in the oxidation ratio of the rock as spilitization proceeds, a change opposite to that which would have been expected. However the changes in mineralogy may sufficiently account for this.

Two further assumptions which have been made in the preceding paragraphs should be considered here: that the spilites have been formed by transformation of basalt and that, this being so, they were formed from basalt of the composition of that in the fresh basalt breccias. Although the true spilites are beautifully fresh and are similar in appearance to spilites which have been considered to be of primary magmatic origin (cf. Benson 1913; Battey 1956) it seems most likely that they are secondary, that they have been formed by the action of hot fluids on already crystalline rock. The spilites show textures strongly

Table 2. Analyses of a series of rocks from Station 5106 illustrating the course of spilitization

No. 1 is a fresh basalt, no. 2 a slightly altered basalt, no. 3 an incompletely spilitized dolerite and no. 4 a true spilite pseudomorphous after variolitic basalt.

	1 5106·21	2 5106·18	3 5106·2	4 5106·7
SiO_2	49·19	49·20	48·32	50·52
Al_2O_3	15·66	15·75	15·17	14·59
Fe_2O_3	3·48	4·14	2·34	1·61
FeO	7·54	6·16	7·05	7·74
MnO	0·20	0·20	0·25	0·26
MgO	6·96	6·60	9·19	7·90
CaO	10·57	10·75	7·81	6·89
Na_2O	3·10	3·50	4·41	5·20
K_2O	0·28	0·04	0·06	0·04
TiO_2	2·02	1·84	1·76	1·86
P_2O_5	0·07	0·13	0·07	0·05
H_2O+	0·78	1·95	3·51	3·26
H_2O-	0·59	0·18	0·41	0·23
	100·44	100·44	100·35	100·15
or	1·65	0·24	0·35	0·24
ab	26·23	29·62	34·96	42·16
an	27·99	27·15	21·42	16·35
ne	—	—	1·28	1·00
ol fo	2·09	1·37	12·72	10·62
ol fa	1·06	0·48	5·25	6·13
hy en	7·95	7·12	—	—
hy fs	3·67	2·26	—	—
di wo	10·02	10·58	7·04	7·31
di en	6·41	7·36	4·74	4·52
di fs	2·96	2·34	1·77	2·36
mt	5·05	6·00	3·39	2·33
il	3·84	3·49	3·34	3·53
ap	0·17	0·31	0·17	0·12
	99·08	98·32	96·44	96·67
water	1·37	2·13	3·92	3·49
	100·45	100·45	100·36	100·16

Table 3. The analyses of table 2 recalculated on the basis of grams of oxide in 100 ml. of rock

	1 5106·21	2 5106·18	3 5106·2	4 5106·7
SiO_2	138·0	139·0	137·8	139·9
Al_2O_3	43·9	44·5	43·3	40·4
Fe_2O_3	9·8	11·7	6·7	4·5
FeO	21·2	17·4	20·1	21·4
MnO	0·6	0·6	0·7	0·7
MgO	19·5	18·6	26·2	21·9
CaO	29·7	30·4	22·3	19·1
Na_2O	8·7	9·9	12·6	14·4
K_2O	0·8	0·1	0·2	0·1
TiO_2	5·7	5·2	5·0	5·2
P_2O_5	0·2	0·4	0·2	0·1
H_2O+	2·2	5·5	10·0	9·0
H_2O-	1·7	0·5	1·2	0·6
density	2·806	2·825	2·851	2·769

PHILOSOPHICAL TRANSACTIONS OF THE ROYAL SOCIETY A MATHEMATICAL, PHYSICAL & ENGINEERING SCIENCES

reminiscent of the fresh basalts, with pseudomorphs that are clearly after olivine, and rounded areas that represent filled vesicles. A replacement origin for the albite is suggested by the veins and grains of chlorite that invade the skeletal felspar crystals. These indications are reinforced by the occurrence of rocks intermediate between fresh basalts and spilites, suggesting that the replacement process has been interrupted at different stages. Finally, dredge hauls from the ocean floor include most commonly fresh basalt (or basalt

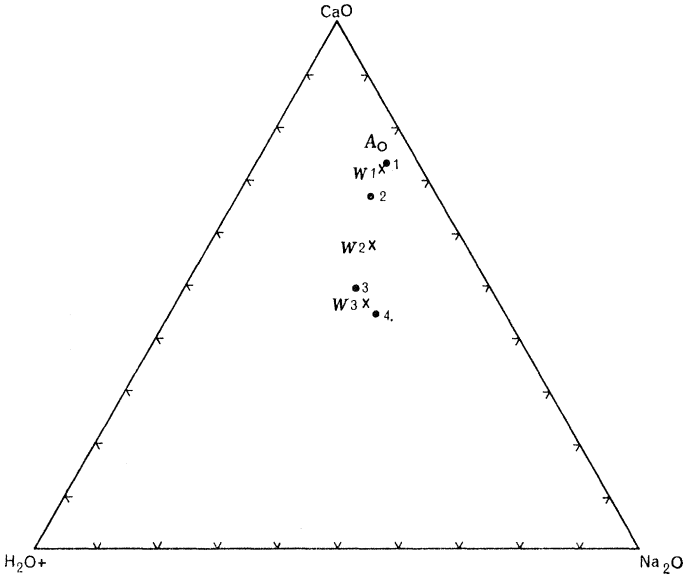

FIGURE 3. Triangular diagram of CaO–Na_2O–H_2O+ on a weight percentage basis for ocean bottom basalts and spilites. *A*, average of 26 fresh ocean floor basalts. 1, 2, 3, 4, rocks described in this paper, corresponding to the analyses of table 2. *W*1, *W*2, *W*3, analyses from Wiseman (1937), *W*1 is table III, no. 1, *W*2 table I, no. 1, *W*3 table V, no. 1.

only affected by submarine weathering), indicating that the crystallization of basalt liquid in the presence of sea water is not enough by itself to give rise to spilites. Fresh basalt has been reported from the oceans at depths up to 4900 m (Korzhinskii 1962).

As far as the second assumption stated above goes, the striking convergence of composition of deep ocean basalts mentioned above, and the fact that the fresh basalt from the breccias belongs to this class, would seem to justify using the fresh basalt breccias as the parent for the spilites at least as far as the comparison is carried here. If this conclusion is granted the series developed here becomes of considerable interest, as this is apparently the first place in which a spilite has been found where the composition of its parental basalt is known with any degree of certainty. Normally spilites are developed over wide areas in continental regions, and although they may be associated with fresh basaltic rock, it cannot be certain that it is from rock of this composition that they have been derived (Vallance 1960). Here we can see more exactly the chemical changes occurring which have before been traceable only in their broad outlines. Figure 3, a triangular diagram of weight percentages of CaO, Na_2O and H_2O+, shows the major variable elements present in the spilites, and on this the course of spilitzation may readily be followed from the average composition of twenty-six fresh deep ocean basalts through the four analyses of table 2.

Although spilites do not seem to have been recorded explicitly from the oceans before, the series of rocks described by Wiseman (1937) from $1\frac{1}{2}^{\circ}$ S on the Carlsberg Ridge in the Indian Ocean includes two specimens wholly or partly spilitized as well as a basalt (which is somewhat weathered and oxidized.) These three specimens have also been plotted on figure 3 and can be seen to fall well on the trend defined by the rocks described here. The petrographic descriptions, which record abundant chlorite and a sodic plagioclase, leave no doubt that these rocks have been subjected to processes of spilitization.

(iii) *Rocks of ultramafic mineralogy*

The three specimens of ultramafic mineralogy all have a finely brecciated appearance in hand specimen and thin section. One specimen is composed almost entirely of green chlorite with subordinate actinolite, although this forms relatively large fragments in the breccia. The second is composed of talc and chlorite in approximately equal amounts, and the third almost entirely of talc with some chlorite. The fragments are relatively coarse-grained and are set in a fine-grained matrix of the same minerals. The identity of the talc has been confirmed by X-ray diffractiometer traces.

The origin of these rocks is probably to be sought in the material of ultrabasic composition which often occurs interstitially to spilitic pillows (Vallance 1965) and seems to represent original basalt glass that has reacted differently from the crystalline rock to the process of spilitization. This conclusion is reinforced by the appearance of one of the spilites, in which the felspar laths, while retaining their unmistakeable shape, have been replaced in many parts of the rock by green chlorite. Such a specimen is probably intermediate between the spilite of the pillows and the ultrabasic material filling the gaps between them.

(iv) *Breccias in process of replacement by quartz*

Perhaps the most remarkable group of specimens from this haul is that of nine rocks which can be arranged in order so that they show the progressive replacement of a breccia of originally ultramafic mineralogy by quartz.

In their least replaced form the rocks are composed of angular to rounded fragments of ultramafic mineralogy set in a matrix of elongate rounded quartz grains embedded in flaky talc and chlorite (figure 13, plate 2). The fragments, which may be up to 1 cm across, show the same variation in mineralogy as do the ultramafic rocks described above, consisting of chlorite, talc and actinolite in varying proportions associated with minor amounts of sphene. The identity of the talc and chlorite has been confirmed by X-ray powder diffractometer traces.

As the replacement proceeds the proportion of quartz in the matrix increases gradually. First it takes on a beautifully euhedral shape (figure 14, plate 3), with the hexagonal cross-sections showing a zoning marked by layers of fine inclusions and a variable extinction position, and then, as the grains grow and eventually come into contact, the euhedral shape is lost and the matrix is almost entirely composed of subhedral quartz with a little remaining chlorite and talc. During the first stages of this process the ultramafic fragments are virtually unaffected except for the growth of rare quartz porphyroblasts, but when the matrix has been almost entirely replaced the fragments themselves are in turn transformed to aggregates of fine grained flaky quartz. The final result is thus a nearly pure quartzite

consisting of rounded to angular areas of flaky quartz in a matrix of larger subhedral grains cut by very coarse grained quartz veins (figure 15, plate 2).

Two specimens, while clearly belonging to this series, show somewhat anomalous features. In one, in which the replacement of the matrix is nearly complete, the fragments are seen to be of spilite rather than the usual ultramafic rocks. In the other, which is equivalent to an earlier stage of the replacement, angular fragments which appear to have been once basalt glass are now composed of fine grained chlorite with a strong preferred orientation, and are being replaced by quartz, epidote and sphene. The texture of the rock suggests a basalt glass being replaced progressively away from joint planes rather than a breccia of glass fragments. The replacing veins, which form a pattern similar to that of jointing in a fine-grained basalt, vary in grain size from microscopically small to about $\frac{1}{4}$ mm, when the grains of epidote and sphene are nearly euhedral.

Although the specimens in the series just described were collected in the arbitrary way which is all dredging allows, the gradual petrographic changes in the rocks leave little doubt that the series represents different stages of a replacement process. The original rocks were probably breccias of fragments of ultramafic mineralogy in a matrix of the same minerals which had probably in turn been derived by the operation of the process of spilitization on breccias of basalt glass fragments similar to those described above. These transformed breccias have suffered a gradual hydrothermal replacement by quartz until the result is a nearly pure quartz rock in which the texture alone would suggest its origin even if there were not a complete intermediate series. Such a chemical change is of a very profound nature, and demonstrates the possibility of the formation of quartz in the oceans far removed from any continental region.

(*c*) *Station* 5123

Three specimens of rock were recovered at station 5123, all of them large and all heavily encrusted and often penetrated by manganese. Only one specimen, the most solid, was sliced, and it was found to be a hornblende gabbro: the other specimens had an identical appearance but were not coherent enough to cut.

Thin sections show the rock to be irregularly banded, with crude lenticular bands of green hornblende alternating with more abundant ones of plagioclase. The areas of hornblende are polycrystalline and the crystals are folded, bent and broken. The plagioclase, of composition An_{50} is similarly crushed and bent. Other lenticular bands, also crushed and fractured, are composed of fine-grained equigranular clinozoisite, and in some patches the hornblende is replaced by foliated green chlorite associated with thin stringers of fine-grained sphene.

The interpretation of the petrography is difficult. The crushing, which even becomes mylonitization in places, clearly follows the formation of all the minerals. However, the association hornblende–labradorite–clinozoisite–chlorite is not in equilibrium and cannot be original. It seems probable that the clinozoisite and chlorite have been formed together during metamorphism in greenschist facies conditions. However, it is not at all clear from what the clinozoisite formed. The labradorite in the section is still quite fresh, and the clinozoisite is not associated with albite as would be expected if it formed from the plagioclase. It is difficult, on the other hand, to propose another mineral which it could have

replaced. The assemblage hornblende–labradorite, assuming this to have existed prior to the greenschist metamorphism, could be a primary igneous assemblage, but the hornblende does not have the appearance of igneous hornblende, and the assemblage might well have formed from a gabbro during relatively high grade amphibolite facies metamorphism.

The history of this specimen is thus clearly complex, and without the possibility of studying its field relations it is impossible to make any more positive statement about its origin.

(*d*) *Conclusions*

All of the rocks from the hauls 5106 and 5123 from the line of hills flanking the fault trough to the southeast have been affected to some extent by crushing and brecciation, metamorphism and hydrothermal activity. The origin of at least some of these features must be sought in connexion with the faulting itself, although the apparent line of the fault lies in the deep northeast–southwest trough several miles away from the haul positions and is separated from them by the crest of the line of hills referred to above. It seems that the specimens collected cannot have been transported to the station positions from the fault trough, and thus that the effects of faulting cannot be localized along that line alone. We appear to be concerned with a broad fault zone, rather than a strictly localized fault, and this conclusion is supported by the magnetic data (see later).

However, although the crushing and brecciation and at least some of the hydrothermal replacement is probably associated with the faulting, the metamorphic effects observed may well not have the same origin. The occurrence of partly spilitized and fresh basalt in adjacent fragments in the fresh basalt breccias is striking. Burial to a depth of about a kilometre or less, coupled with a rise in temperature to about 200 °C would bring the rocks into the lower greenschist facies of metamorphism, such as is exemplified by the spilites. As such conditions would not be at all unlikely beneath the surface of the ridge, the action of the fault would have been simply to bring already metamorphosed rocks to the ocean floor. There is every reason to expect that similar metamorphic processes would take place very generally at some depth beneath the ocean floor, particularly within ridge structures where the temperature gradient beneath the sea floor appears on the average to be rather greater than elsewhere.

The elongate seamount from which the haul (5111) containing fresh basalt pillows was made and on which two camera stations showed the presence of abundant pillow lava outcrops cuts across the line of the hills flanking the fault trough, and can best be explained as a recent volcano, post-dating the faulting and concomitant brecciation.

Finally it should be pointed out that the minerals of the metamorphosed and hydrothermally altered rocks, quartz, albite, epidote, chlorite, sphene, hornblende, actinolite and talc, which are normally considered to be of continental origin, have been demonstrated to occur in place on the sea floor, and might well be found in deep-sea sediments close to their point of origin. Of these minerals, chlorite, epidote, sphene and perhaps actinolite have been reported by Heezen, Bunce, Hersey & Tharp (1964) from sediments in the Romanche Trench and perhaps the Vema trench, and probably originate in rocks similar to those described above. Quartz, albite and talc have yet to be recorded from such sediments, but they may well be present. Conversely, the presence of such

minerals suggests that rocks similar to those described could probably be recovered from the Romanche and Vema Trenches, and perhaps from other transverse fractures as well.

Age determinations

Whole-rock potassium-argon age determinations have been made on several of the dredge samples by Dr R. L. Grasty of the Department of Geodesy and Geophysics, Cambridge. They suggest that the rocks are very young geologically in that all the results were of Pliocene or Pleistocene age. Despite great care and repeated determinations it is not possible to be more specific than this because the potassium content of the rocks is so low. The results are comparable to those obtained from dredged rocks in an analogous area on the Mid-Atlantic Ridge (Muir & Tilley 1964).

Magnetic survey

(*a*) *Instrumentation*

Virtually complete total magnetic field records were obtained throughout the survey. The proton precession magnetometer towed by the ship (Hill 1959) was cycled at 1 min intervals, and the readings recorded digitally on punched tape, and in analogue form on a pen recorder. In addition, a further magnetometer (Mason 1963), which was incorporated in an anchored buoy, gave a continuous record of diurnal variation throughout the period of the survey.

(*b*) *Reduction*

The punched tape output from the ship-borne magnetometer has subsequently been processed on a computer by means of a reduction program written by Bullard (1960). The program converts each magnetometer reading to total magnetic field, corrects for diurnal variation and the magnetic effect of the ship, removes a regional trend, smooths, and interpolates the resulting anomalies at equal intervals of time.

The daily variation curves used in the reduction were those obtained from the buoy magnetometer record, modified, with the aid of synchronous records from Aden and Bombay in order to reduce errors arising from slight buoy drift in an area of considerable magnetic gradient (Mason 1963). The coefficients used in the expression for ship's heading correction (Bullard & Mason 1961) were derived from an experimental determination of the magnetic effect of the ship, performed around an anchored buoy to the northeast of the Seychelles. The correction applied is given by

$$\Delta F = 9 - 7{\cdot}5 \cos\theta + 13{\cdot}5 \cos 2\theta - 1{\cdot}2 \sin\theta \ (\gamma),$$

where θ is the ship's magnetic heading; ΔF being subtracted from the observed field. Although these coefficients vary considerably with magnetic latitude and probably with time, calculations have shown that the amplitude of the effect is essentially the same for the survey area, and that the zero shift is small, and since it is a constant field, is therefore unimportant. The regional gradient removed is a planar approximation to the third-order polynomial fitted to magnetic profiles obtained over the Arabian Sea, by sea and air prior

to January 1962 (Bullard 1963); its absolute value, however, is 150 γ less than this. Thus the regional trend removed is given by

$$F = 37325 + 1{\cdot}9N + 2{\cdot}5E\ (\gamma),$$

where N and E are minutes of latitude and longitude north and east of 4° 50′ N and 61° 15′ E. The maximum discrepancy between this gradient and the polynomial field in the survey area is 5 γ.

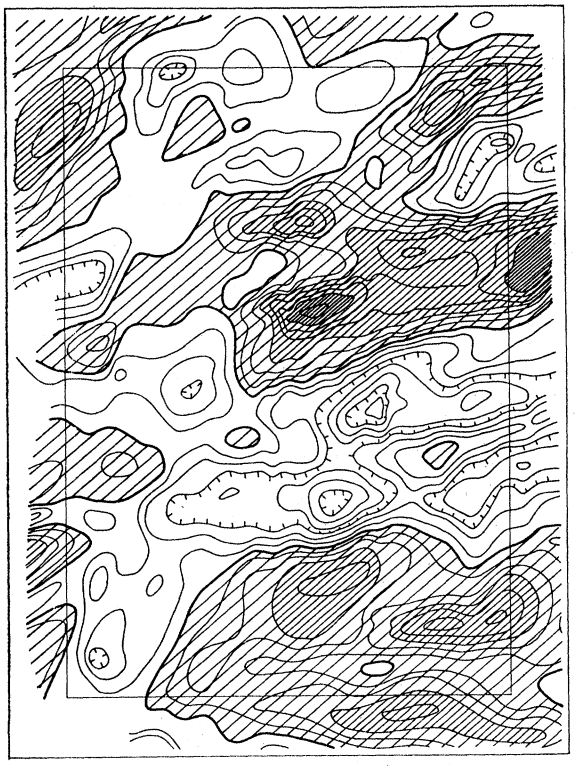

FIGURE 4

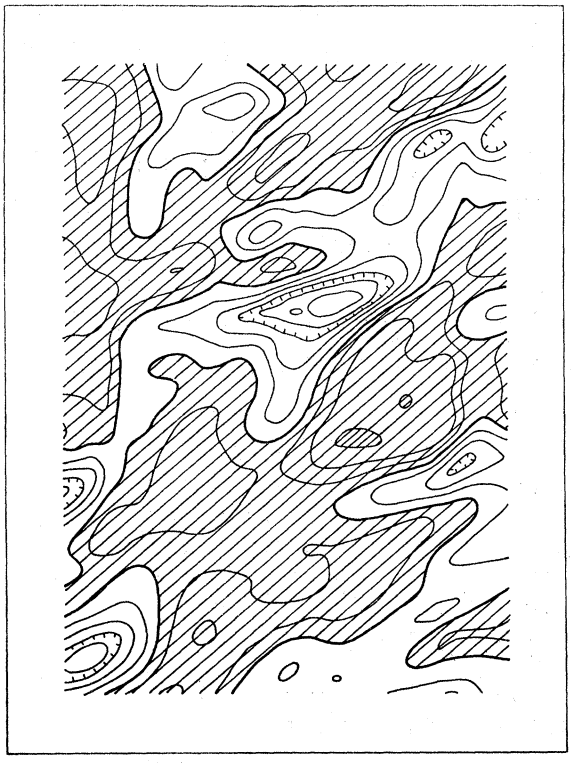

FIGURE 5

FIGURE 4. Observed magnetic anomalies, contour interval is 50γ (1γ = 10^{-5} Oe). Positive anomaly areas are shaded; shading interval is 150γ. Shading lines run east–west. Inner rectangle indicates the area covered by the computed anomaly maps.

FIGURE 5. Map of computed magnetic anomalies for normal induced magnetization assuming a susceptibility of 0·0133. Bearing and inclination of the Earth's field = 356°; −6° (up). (See legend to figure 4 for convention.)

The resulting contour map of total field anomalies (figure 4) is probably unique in its accuracy and detail for an area over the deep ocean.

(*c*) *Description of anomaly map*

Leaving aside the faulted area to the left (figure 4), it is striking that the magnetic anomalies exhibit a marked elongation paralleling the trend of the Ridge, regardless of the bathymetry (figure 2). In figure 4 the central positive and negative anomalies persist to the right despite the complete change in bathymetry along their lengths. This negative anomaly is, in fact, the large central anomaly observed over the crest of the Ridge (Vine & Matthews 1963; Matthews *et al.* 1965).

PHILOSOPHICAL TRANSACTIONS OF THE ROYAL SOCIETY A MATHEMATICAL, PHYSICAL & ENGINEERING SCIENCES

Here, over the crest of the Ridge, the bottom topography suggests basic extrusives, such as volcanoes and fissure eruptives, and there is little sediment fill. The bathymetry therefore defines the upper surface of magnetic material having a considerable intensity of magnetization, potentially as high as that of any known igneous rock type (Bullard & Mason 1963). One would therefore expect there to be some correlation between the topography and the magnetic anomalies. In places this is so; the central seamounts for example, have associated positive anomalies, and the isolated seamount in the top right (figure 2) also has an anomaly pattern associated with it. In other places, however, there are very steep magnetic gradients over essentially flat topography.

(*d*) *Computations and simulated anomaly maps*

Assuming that the magnetic material represented by the bathymetry is uniformly magnetized in the present direction of the earth's field, an anomaly map has been computed for the central part of the area and is presented here as figure 5. Throughout, computed anomaly maps cover an area of 43×31 mi., and anomalies being computed at points on a grid of 1 mi. squares. In computing anomalies at points within a central area of 35×23 mi., 256 sq.mi. of bathymetry around each point were taken into consideration. Outside this central area, anomalies at points within the remaining border, 4 mi. in width, were computed by considering the bathymetry within 64 sq.mi. around each point. The method of computation is analogous to that suggested by Bott (1963), having approximated the bathymetry by vertical square prisms, 1 sq.mi. in cross-sectional area. In all the computations, the intensity of magnetization has been taken as 0·005 e.m.u., irrespective of the direction of magnetization. Thus in the case of normal induced magnetization (figure 5), this is equivalent to a susceptibility of 0·0133. Despite this very high susceptibility, the amplitudes and gradients of the computed anomalies are clearly too small, and correlation with the observed anomalies, where it occurs, is often inverse (it is interesting to note that the most pronounced feature on the bathymetric chart, the scarp flanking the fault trough, produces very little effect because it runs approximately north–south, and the earth's field is almost horizontal).

In order to continue with reasonably objective interpretation, it was next decided to apply a 'vector fitting' technique. Where comparatively isolated seamounts clearly have associated anomalies, one can, by means of a computer, assume that the seamount is uniformly magnetized and fit a vector to it such that the resulting computed anomaly gives the best least squares fit with the anomaly observed over the seamount. This technique was applied to the central seamount and the isolated seamount in the top right of figure 2. In each case, the observed anomalies at 60 points above the seamount were taken into consideration, and the contours of the seamount were approximated at 100 fm. intervals to a depth of 1500 fm. The resulting vectors are shown in figure 6. The almost perfectly reversed vector was obtained for the central seamount.

This method was then extended to the whole of the central area of the survey (figure 7). At each point on this grid, taking into account the observed anomaly at that point and at eighty others around it, the computer has fitted a vector to the volcanics represented by the bathymetry, assuming that they are uniformly magnetized.

Many of these vectors are approximately reversed with respect to the present direction

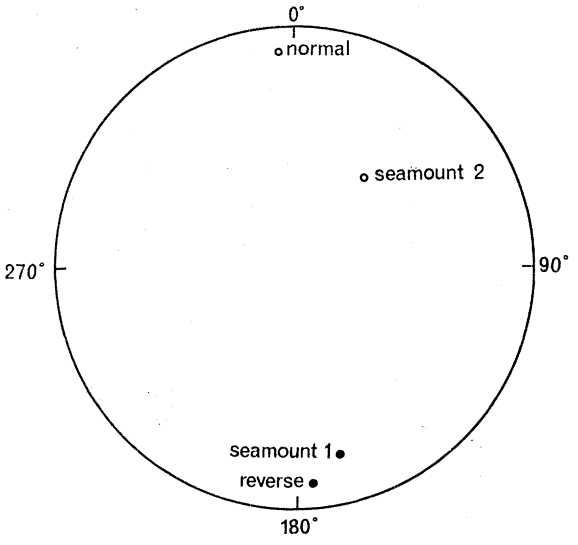

FIGURE 6. Stereographic plot of the magnetic vectors obtained from the two isolated seamounts, together with the direction of the present earth's field and its reverse. Bearings and inclinations: present field vector (normal) 356°; −6° (up); fitted vectors: seamount 1, 166° 30′; +13° (down); seamount 2, 038°; −40° (up).

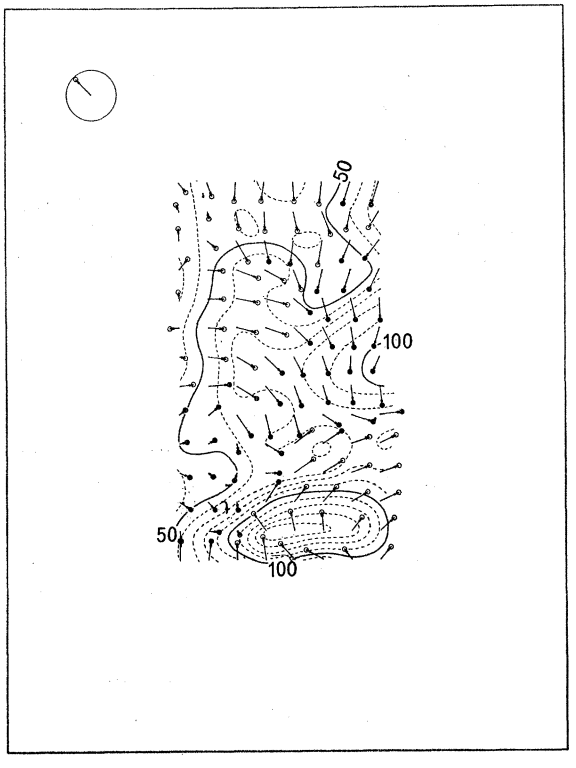

FIGURE 7. Vectors fitted at 112 points over the central part of the area by considering the observed anomaly about each point and assuming that the material represented by the bathymetry is uniformly magnetized. The vectors are plotted stereographically and in the top left-hand corner the present field vector has been plotted together with the primitive. The frame is equivalent to that of all the other figures and represents the area of 51 × 39 mi. The background contours give an indication of the 'goodness of fit' in that they represent the root mean square of the residuals (residual = observed anomaly − calculated anomaly assuming fitted vector). Contour interval is 10γ.

PHILOSOPHICAL TRANSACTIONS OF THE ROYAL SOCIETY A MATHEMATICAL, PHYSICAL & ENGINEERING SCIENCES

of the Earth's field. In the lower part of the grid, they begin to swing round, but, as is suggested by the background contours, the fit is very much worse, and the vectors are not therefore very meaningful; on the map of observed anomalies this is an area of very steep magnetic gradient which is uncorrelated with topography.

This work did at least give an indication of the resultant intensity of magnetization of the surface rocks, which was consistently about 0·005 e.m.u. and this intensity, as mentioned previously, has been used throughout the calculations.

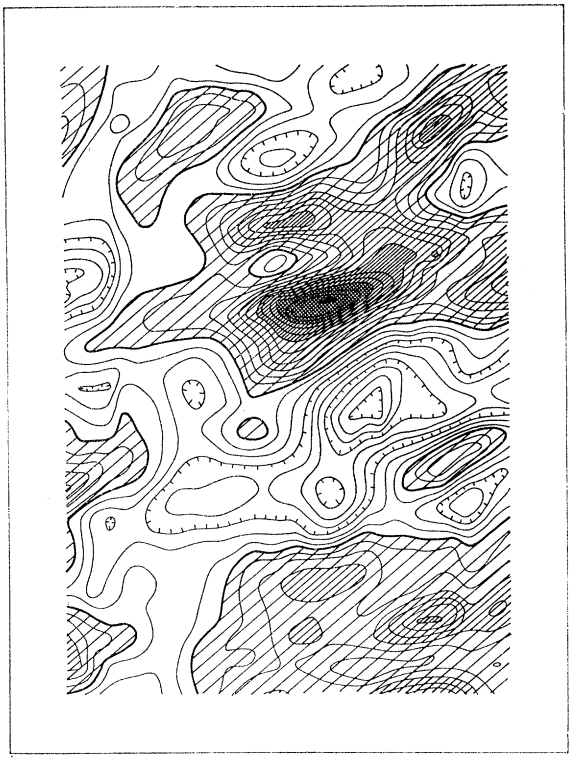

FIGURE 8

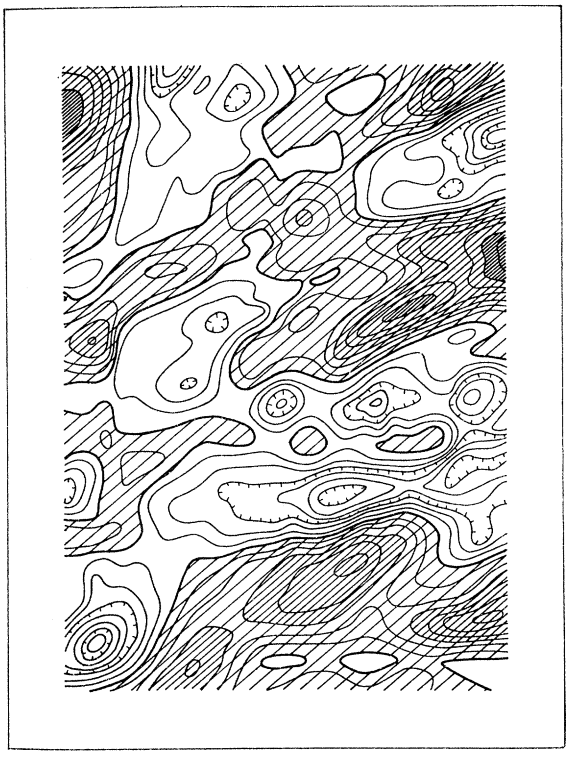

FIGURE 9

FIGURE 8. Map of residuals. At each point the anomaly due to the bathymetry, assuming uniform normal magnetization with respect to the axial dipole field, has been subtracted from the observed anomaly at that point. (Convention as for figure 4.) Axial dipole dip taken as +10° 45′ (down).

FIGURE 9. Cf. figure 8. Map of residuals, having removed the effect due to uniform reverse magnetization of the bathymetry, from the observed anomalies. (Convention as for figure 4.)

Thus, one is clearly not dealing with induced magnetization; this is hardly surprising in that the basic volcanics involved are known to have ratios of remanent to induced magnetization of the order of 20, with a range possibly from 2 to 400. Moreover, there is some evidence to suggest that this remanence is sometimes reversed in direction with respect to the present direction of the earth's field. If current ideas about this crestal part of the ridge are correct, it is comparatively young geologically, and one would expect any remanent magnetization to be either essentially normal or reversed with respect to the axial dipole field (that is, the mean of secular variations, as assumed in palaeomagnetic work).

PHILOSOPHICAL TRANSACTIONS OF THE ROYAL SOCIETY A MATHEMATICAL, PHYSICAL & ENGINEERING SCIENCES

If one assumes that the topography is uniformly magnetized, such that its resultant magnetization is (*a*) normal and (*b*) reversed, and removes each of these effects in turn from the map of observed magnetic anomalies, one obtains the maps presented in figures 8 and 9. It must be emphasized that these are maps of residuals, having attempted a topographic correction. The case of 'normal removed' (figure 8) is analogous to a correction for the induced component of magnetization, but is probably at least one order of magnitude too great since the intensity assumed is the 'resultant intensity' (remanent+induced) obtained from the vector fitting technique; clearly such a correction for induced magnetization would be negligible.

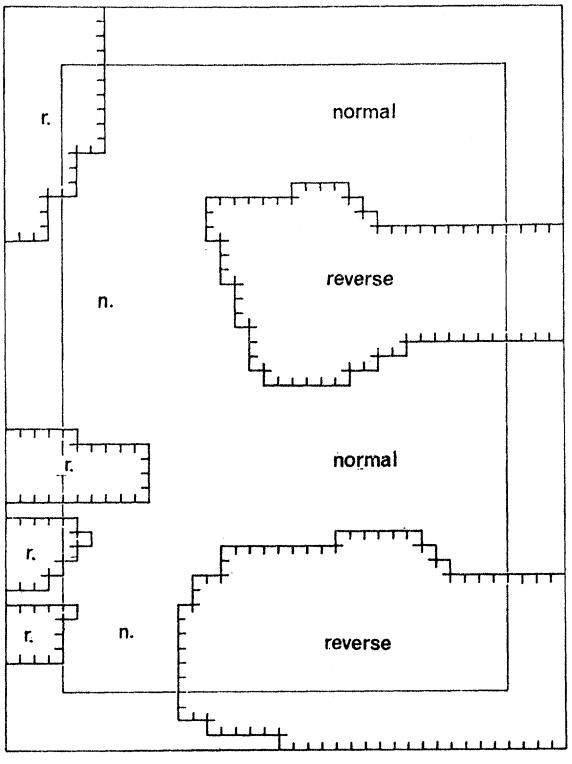

FIGURE 10

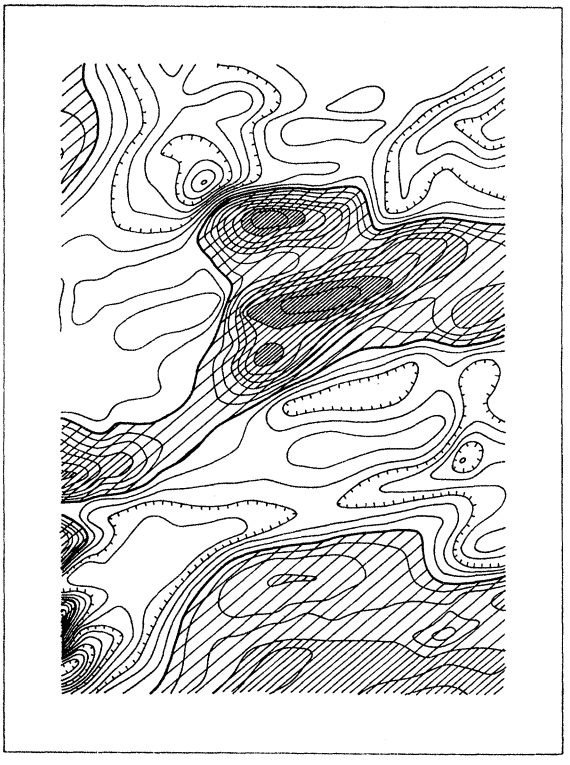

FIGURE 11

FIGURE 10. Diagram of the area showing the way in which it was divided into blocks of normally and reversely magnetized material for the simulation presented in figure 11. Inner rectangle indicates the area covered by the computed map.

FIGURE 11. Simulated anomaly map assuming that the area is divided into blocks of normally and reversely magnetized material as outlined in figure 10. Intensity of magnetization taken as 0·005 e.m.u. 'Normal' or 'Reverse' magnetization with respect to axial dipole field; dip taken as $+10°\ 45'$ (down).

On both maps (figures 8 and 9), anomalies and gradients are reduced in certain areas but increased in others. In neither, is the distinct lineation of the anomalies destroyed.

One cannot therefore make a simple topographic correction. The magnetic effect of the topography is inextricably bound up with anomalies due to contrasts within it. One has therefore, at this stage, to postulate some model, which will inevitably be subjective, because of the many parameters involved.

On the basis of this work, it was decided to try a very simple model, in which the area is divided into blocks (figure 10) of normally and reversely magnetized material of the same intensity of magnetization, uniform throughout each block. The blocks extend down to the greatest depth in the area, 2·2 mi. The computed anomaly map obtained from this very crude and simple model is presented in figure 11.

(*e*) *Discussion*

Only two *simulations* have been presented—in figures 5 and 11—and these should be compared with figure 4, the map of observed anomalies. On comparing figures 4 and 11, it is apparent that although the simulated anomalies fit well in the region of the central negative anomaly, the amplitude of the simulated anomaly is considerably less than that which is observed. The discrepancy could be reduced by increasing the resultant intensity of magnetization of the underlying 'normal block'. Two-dimensional computations suggest that this intensity must at least be doubled to simulate the observed amplitude.

The steepest gradient in figure 11 occurs in the region of the two dredge hauls, 5106 and 5123, which contained exclusively brecciated rocks, often with modified mineralogy. As has been noted elsewhere (Matthews *et al.* 1965), the brecciation and alteration of rocks within a comparatively wide zone associated with such a transcurrent fault, would appear to reduce the net magnetization of the crustal rocks, in that such areas are typically devoid of the strong magnetic relief normally associated with the crest of the ridge. This is amply borne out in this area. The third dredge haul, 5111, was obtained on the flanks of the central seamount, and yielded fresh, unaltered basalt lavas. Over this feature, the simulated anomaly is a fairly good approximation to the observed.

In comparing figures 4 and 11, two further points seem worthy of notice. Despite the choice of blocks paralleling the trend of the ridge, the elongation of the anomalies on the observed map is still greater than that on the simulated map, suggesting that within the blocks there are structures, probably fissures, paralleling the trend of the Ridge, not necessarily reflected in the topography, but controlling the magnetic contrasts. Clearly, since the survey was carried out at a height of about 10000 ft. above the mean depth on the area, the anomalies due to individual dykes and fissure eruptions are attenuated and combined to give, approximately, the overall effect of a 'block' of essentially normal or reversed material, according to the time of formation.

It is also apparent from the survey area, although most marked on any profile crossing the Ridge, that this very crude model only really succeeds at the centre of the Ridge, in the region of the central anomaly. If one assumes an ocean floor spreading hypothesis (Hess 1962), then the formation of new oceanic crust (layer 3) almost certainly only occurs at one place, that is within the central block, at any one time. However, it seems probable that extrusion and intrusion of basaltic material (layer 2) occurs over a much wider area, producing minor crustal extension due to dyke formation, and building up lava flows and volcanoes. Extrusions and intrusions away from the central block may well account, in part at least, for the central depression or valley, where developed. On the basis of this model, only the central 'block' will be composed exclusively of young material which is magnetized normally (i.e. approximately parallel to the present direction of the axial dipole field) except for the minor probability of self reversals. All other blocks will be

PHILOSOPHICAL TRANSACTIONS OF THE ROYAL SOCIETY A MATHEMATICAL, PHYSICAL & ENGINEERING SCIENCES

contaminated with younger material, often of reverse polarity to that of the initial block, and hence lowering or modifying its resultant magnetic effect.

This interpretation, in terms of ocean floor spreading and periodic reversals in the Earth's magnetic field, has been published previously on the basis of preliminary, mainly two-dimensional, computations (Vine & Matthews 1963). It will be noted that in the computations presented here, the magnetic material has only been considered to a depth of 2·2 mi., whereas in the previous paper, generalized 'crustal blocks' extending from 1·6 to 6 mi. were used over the crests of ridges to simulate the observed anomalies. This is not really as different as it seems. The basic tenet of the idea, is the combination of ocean-floor spreading and periodic reversals, which provides a plausible and effective mechanism to produce a considerable magnetic contrast across an approximately vertical boundary within the oceanic crust, without implying any change laterally in the petrology of the crustal material. Such boundaries would appear to be essential if one is to simulate the steep magnetic gradients so often observed over the oceans, and notably at the centre of ridges. Having accepted this basic principle, there is no difficulty in explaining the anomalies, but only in deciding on the distribution of magnetization within layers 2 and 3 of the oceanic crust.

At the two extremes, it is possible to explain the anomalies in terms of blocks confined to layer 2 only, or to layer 3 only. In a general way a thin strongly magnetized layer at comparatively shallow depth, will produce a similar effect to a thick, less strongly magnetized layer at greater depth. For layers 2 and 3 alone, apparent susceptibilities of $\pm 0{\cdot}02$ and $\pm 0{\cdot}005$ respectively, will produce the observed amplitudes. It seems more probable, however, that the anomalies are produced by a combination of the two. Vector fitting results, detailed here and elsewhere, suggest that the apparent susceptibility of layer 2 features is rather less than 0·02, and it seems reasonable to assume that the crustal material beneath layer 2, although coarser grained, and possibly less strongly magnetized, will contribute to the observed anomalies in some way. If this crustal layer is serpentinite as suggested by Hess (1962), it would appear that it is likely to be quite weakly magnetized, with a ratio of remanent to induced magnetization of approximately 1 (Cox, Doell & Thompson 1964). However, it would still be capable of contributing to the anomalies, the bulk of which could be attributed to layer 2.

This attempt to explain the central anomaly so commonly observed over oceanic ridges has been variously described as improbable, startling (Talwani 1964) and fruitful (Hess 1964). It remains, however, as the only detailed explanation in print, despite the fact that a decade has passed since the anomaly was first observed. Clearly, the central anomaly alone can be reproduced if it is assumed that the median valley is underlain by a rectangular block, strongly magnetized in the present direction of the Earth's field, but it is not clear why this central block should be so different from the remaining oceanic crust in producing such a high magnetic contrast with it.

It has been suggested that the central anomaly might be due to a magnetic body at depth, the extent of which is controlled by variations in the depth to the Curie point isotherm (Talwani, Heezen & Worzel 1961). It seems inconceivable that this, or any other effect at depth (for example, local depressions or elevations of the Curie point isotherm), could account for the steep magnetic gradients and short wavelengths of the observed

PHILOSOPHICAL TRANSACTIONS OF THE ROYAL SOCIETY A MATHEMATICAL, PHYSICAL & ENGINEERING SCIENCES

anomalies. As mentioned previously such suggestions are unsubstantiated by detailed models or computations.

The mechanism put forward here might well account for the enigmatic, but possibly ubiquitous, lineation or 'grain' of magnetic anomalies, first observed in the eastern Pacific (Mason 1958; Vine & Matthews 1963). If one were to assume that the average width of these anomalies (i.e. half-wavelength) is 20 km (approximately 10 mi.), and that a major reversal of the earth's magnetic field occurs once every million years (Cox, Doell & Dalrymple 1964), then the model implies a rate of spreading of 2 cm/y for each limb of the spreading system or in the case of the Atlantic, say, a rate of opening of 4 cm/y. If the opening-up has occurred within the last 150 My then this rate of spreading implies a width of 6000 km. Clearly such rough calculations show that the model is consistent with other heretical ideas on ocean-floor spreading and continental drift.

If linear anomalies do parallel existing and extinct oceanic ridges, as this model would suggest, it will clearly be invaluable in deducing the history of the ocean basins, and in resolving the differential spreading on either side of the apparent large transcurrent faults which transect the ocean floor. A further corollary of the model is that ridges over which the central anomaly is consistently absent, might well be inactive, minor basaltic extrusions having post-dated the last phase of crustal emplacement and spreading, or alternatively, so young that spreading has not, as yet, been initiated.

The authors are indebted to the long-suffering officers, crew and scientists of H.M.S. *Owen* and R.R.S. *Discovery*, and in particular to the senior scientists present, Dr D. H. Matthews and Dr M. N. Hill, F.R.S., respectively, for the surveys and dredge samples. The authors also wish to thank Dr H. H. Hess of Princeton University for helpful discussions.

References (Cann & Vine)

Battey, M. H. 1956 The petrogenesis of a spilitic rock series from New Zealand. *Geol. Mag. Lond.* **93**, 89–110.

Benson, W. N. 1913 Spilite lavas and radiolarian rocks from New South Wales. *Geol. Mag. Lond.* (Decade 5), **10**, 17–21.

Bott, M. H. P. 1963 Two methods applicable to computers for evaluating magnetic anomalies due to finite three-dimensional bodies. *Geophys. Prosp.* **11**, 292–299.

Bullard, E. C. 1960 The automatic reduction of geophysical data. *Geophys. J.* **3**, 237–243.

Bullard, E. C. 1963 The total magnetic force in the north–west Indian Ocean. In *Admiralty Mar. Sci. Publ.* no. 4, part 1, 18–21.

Bullard, E. C. & Mason, R. G. 1961 The magnetic field astern of a ship. *Deep-Sea Res.* **8**, 20–27.

Bullard, E. C. & Mason, R. G. 1963 The magnetic field over the oceans. In *The sea* (ed. M. N. Hill), **3**, chap. 10. New York and London: Interscience.

Cox, A., Doell, R. R. & Dalrymple, G. B. 1964 Reversals of the earth's magnetic field. *Science*, **144**, 1537–1543.

Cox, A., Doell, R. R. & Thompson, G. 1964 Magnetic properties of serpentinite from Mayaguez, Puerto Rico. In *A study of serpentinite* NAS–NRC Publ. no. 1188, 49–60.

Davis, B. T. C. & England, J. L. 1964 Melting of forsterite up to 50 kilobars. *J. Geophys. Res.* **69**, 1113.

Engel, C. G. & Engel, A. E. J. 1963 Basalts dredged from the North-Eastern Pacific Ocean. *Science*, **140**, 1321–1324.

PHILOSOPHICAL TRANSACTIONS OF THE ROYAL SOCIETY A MATHEMATICAL, PHYSICAL & ENGINEERING SCIENCES

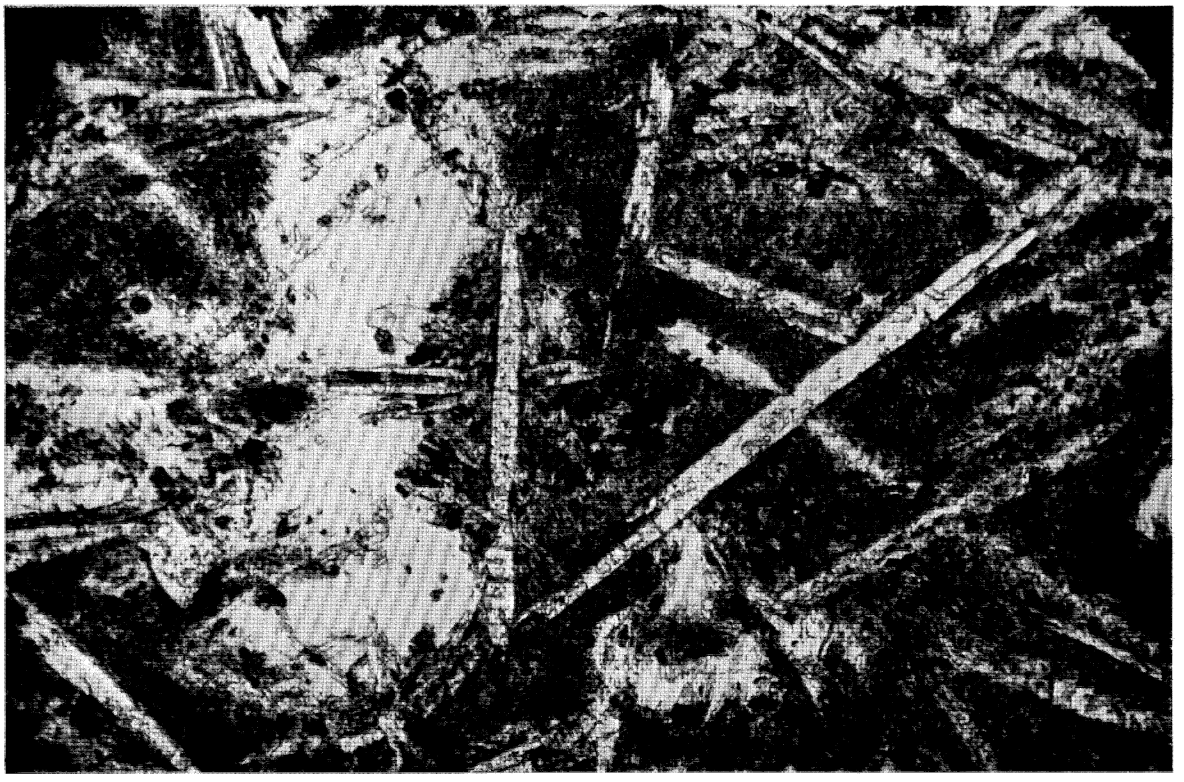

FIGURE 12. A spilite pseudomorphing a variolitic basalt. This is the analysed specimen 4 of tables 2 and 3. Ordinary light; magn. × 50.

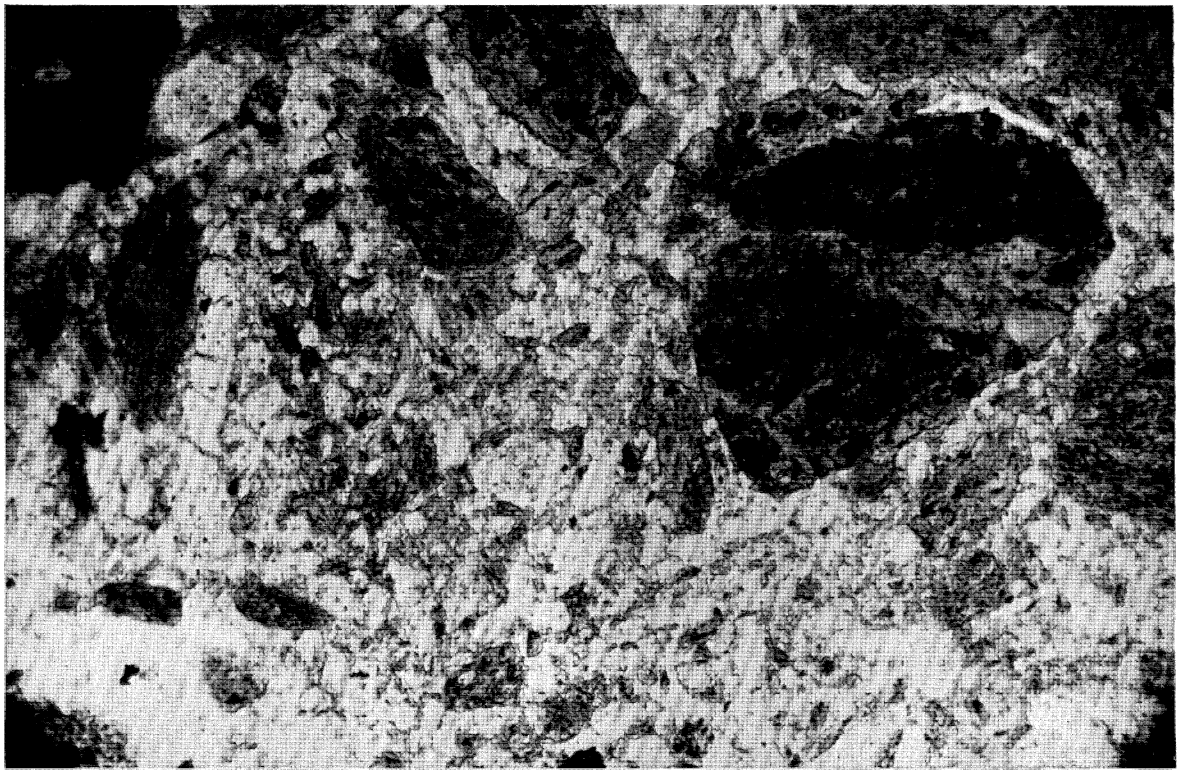

FIGURE 13. An early member of the series in which a breccia of ultramafic mineralogy is replaced by quartz. Rounded fragments of ultramafic mineralogy are set in a ground mass of rounded elongate quartz grains enclosed by flaky chlorite and talc. Ordinary light; magn. × 50.

(*Facing p.* 216)

PHILOSOPHICAL TRANSACTIONS OF THE ROYAL SOCIETY A MATHEMATICAL, PHYSICAL & ENGINEERING SCIENCES

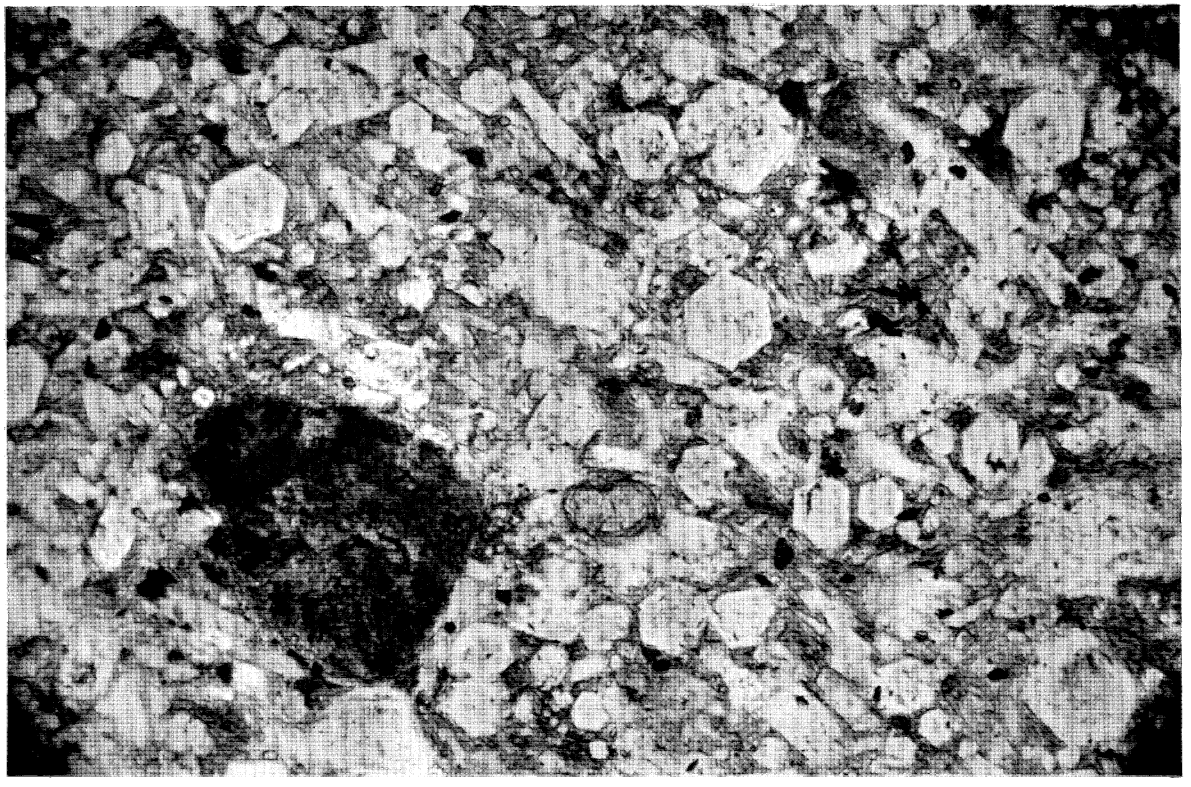

FIGURE 14. An intermediate stage in the replacement of a breccia of ultramafic mineralogy by quartz. The matrix to the ultramafic fragments is composed of euhedral quartz grains set in a base of chlorite and talc. Ordinary light; magn. × 50.

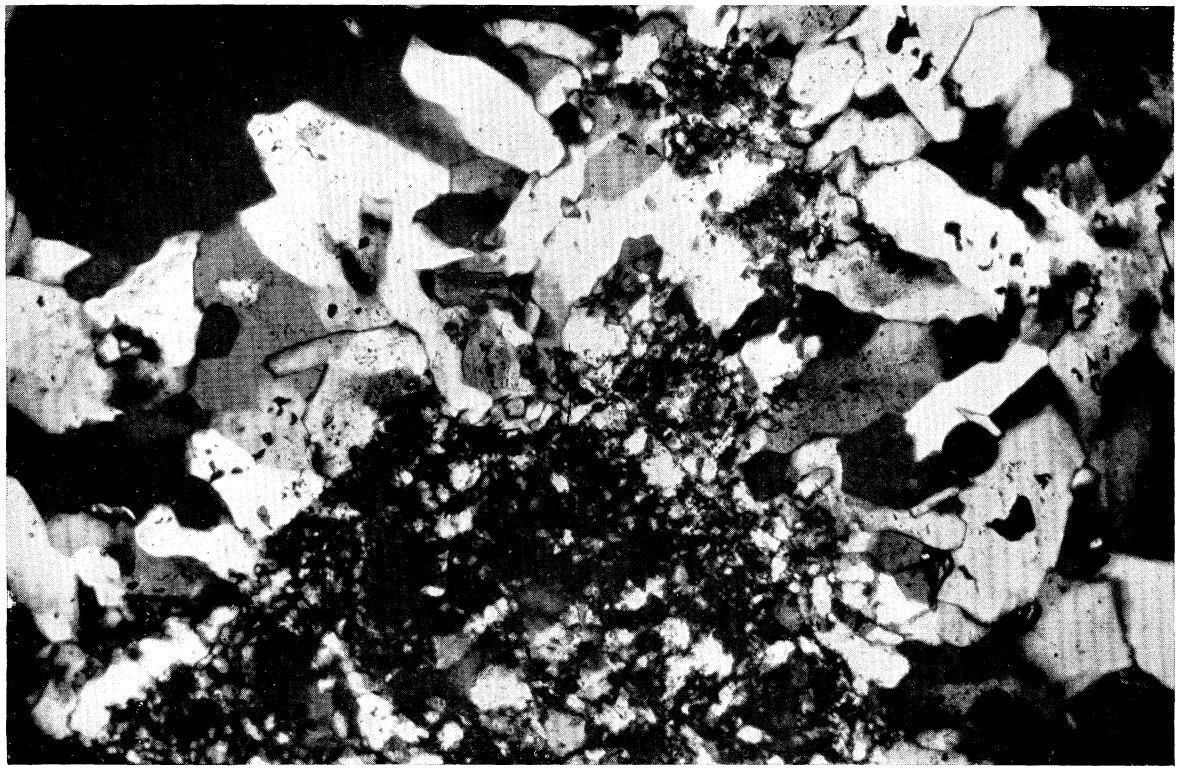

FIGURE 15. The final stage of replacement of a breccia of ultramafic mineralogy by quartz. The area of fine-grained flaky quartz represents the original breccia fragments. The matrix is composed of coarser subhedral quartz crystals. Crossed polars; magn. × 50.

PHILOSOPHICAL TRANSACTIONS OF THE ROYAL SOCIETY A MATHEMATICAL, PHYSICAL & ENGINEERING SCIENCES

Engel, C. G. & Engel, A. E. J. 1964*a* Composition of basalts from the Mid-Atlantic Ridge. *Science*, **144**, 1330–1333.

Engel, C. G. & Engel, A. E. J. 1964*b* Igneous rocks of the East Pacific Rise. *Science*, **146**, 477–486.

Heezen, B. C., Bunce, E. T., Hersey, J. B. & Tharp, M. 1964 Chain and Romanche fracture zones. *Deep-Sea Res.* **11**, 11–35.

Hess, H. H. 1962 History of ocean basins. In *Petrologic studies*, pp. 599–620. Buddington Vol. Geol. Soc. Amer.

Hess, H. H. 1964 Seismic anisotropy of the uppermost mantle under the oceans. *Nature, Lond.*, **203**, 629–631.

Hey, M. H. 1954 A new review of the chlorites. *Miner. Mag.* **30**, 277–292.

Hill, M. N. 1959 A ship-borne nuclear-spin magnetometer. *Deep-Sea Res.* **5**, 309–311.

Korzhinskii, D. S. 1962 The problem of spilites and the transvaporization hypothesis in the light of new oceanological and volcanological data. *Izv. Acad. Sci. USSR*, **9** (Geol. Series), 12–17.

Mason, C. S. 1963 Magnetic measurements at sea. Unpublished Ph.D. dissertation, University of Cambridge.

Mason, R. G. 1958 A magnetic survey off the west coast of the United States (lat. 32–36° N; long. 121–128° W). *Geophys. J.* **1**, 320–329.

Matthews, D. H., Vine, F. J. & Cann, J. R. 1965 Geology of an area of the Carlsberg Ridge. *Bull. Geol. Soc. Amer.* **76**, 675–682.

Muir, I. D. & Tilley, C. E. 1964 Basalts from the northern part of the rift zone of the Mid-Atlantic Ridge. *J. Pet.* **5**, 409–434.

Nicholls, G. D., Nalwalk, A. G. & Hays, E. E. 1964 The nature and composition of rock samples dredged from the Mid-Atlantic Ridge between 22° N and 52° N. *Marine Geol.* **1**, 333–343.

Talwani, M. 1964 A review of marine geophysics. *Marine Geol.* **2**, 29–80.

Talwani, M., Heezen, B. C. & Worzel, J. L. 1961 Gravity anomalies, physiography and crustal structure of the Mid-Atlantic Ridge. *Trav. Scient. Sect. Seism.* U.G.G.I. Ser. A, **22**, 81–111.

Vallance, T. G. 1960 Concerning spilites. *Proc. Linn. Soc. N.S.W.* **85**, 8–52.

Vallance, T. G. 1965 On the chemistry of pillow lavas and the origin of spilites. *Miner. Mag.* (in the Press).

Vine, F. J. & Matthews, D. H. 1963 Magnetic anomalies over oceanic ridges. *Nature, Lond.*, **199**, 947–949.

Wiseman, J. D. H. 1937 Basalts from the Carlsberg Ridge, Indian Ocean. *Report of the John Murray Expedition, 1933–34*, vol. III, 1. London: British Museum (Nat. Hist.).

Yoder, H. S. & Tilley, C. E. 1962 Origin of basalt magmas: an experimental study of natural and synthetic rock systems. *J. Pet.* **3**, 342–532.

PHILOSOPHICAL TRANSACTIONS OF THE ROYAL SOCIETY A MATHEMATICAL, PHYSICAL & ENGINEERING SCIENCES

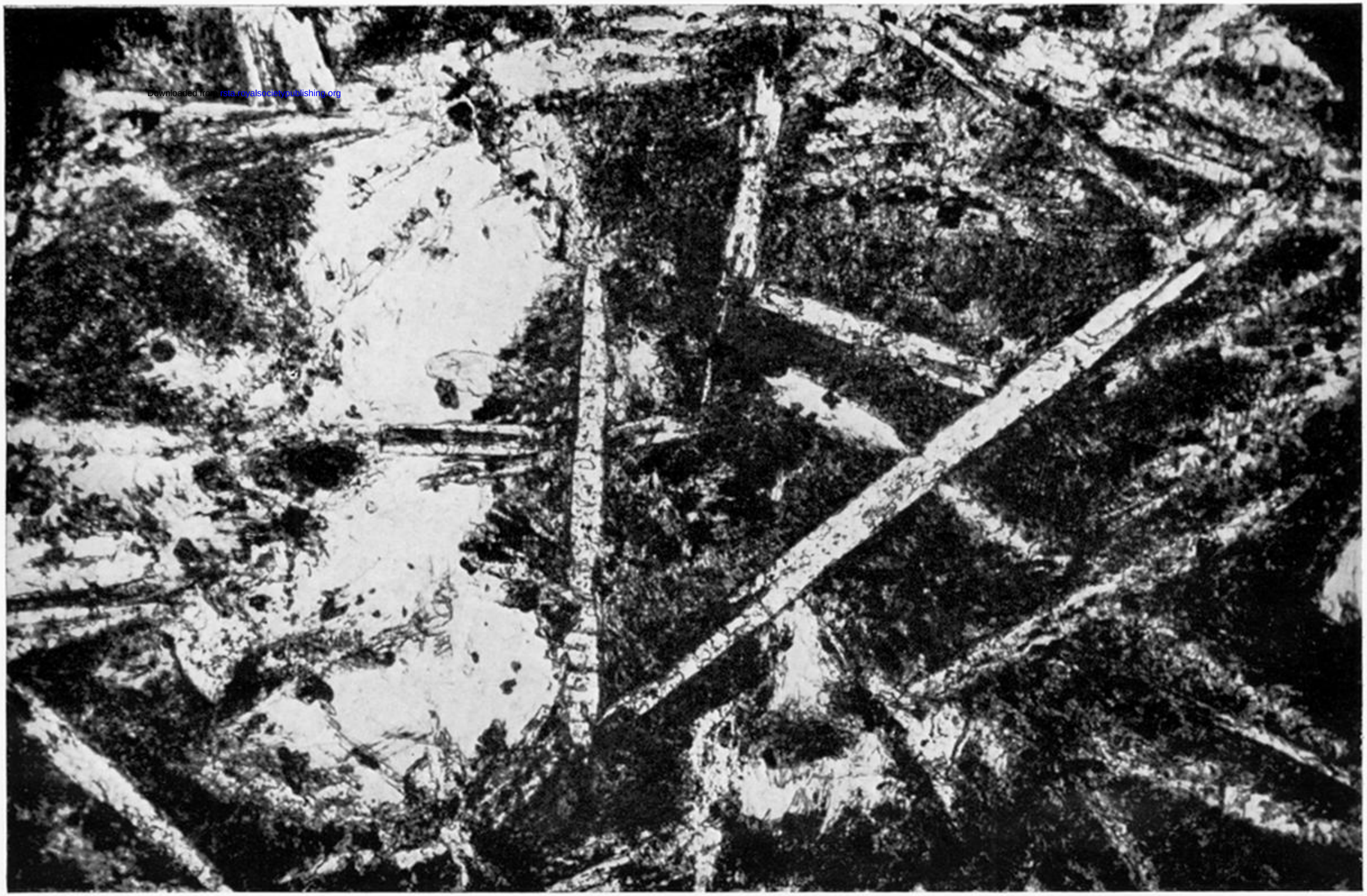

FIGURE 12. A spilite pseudomorphing a variolitic basalt. This is the analysed specimen 4 of tables 2 and 3. Ordinary light; magn. $\times 50$.

PHILOSOPHICAL TRANSACTIONS OF THE ROYAL SOCIETY A MATHEMATICAL, PHYSICAL & ENGINEERING SCIENCES

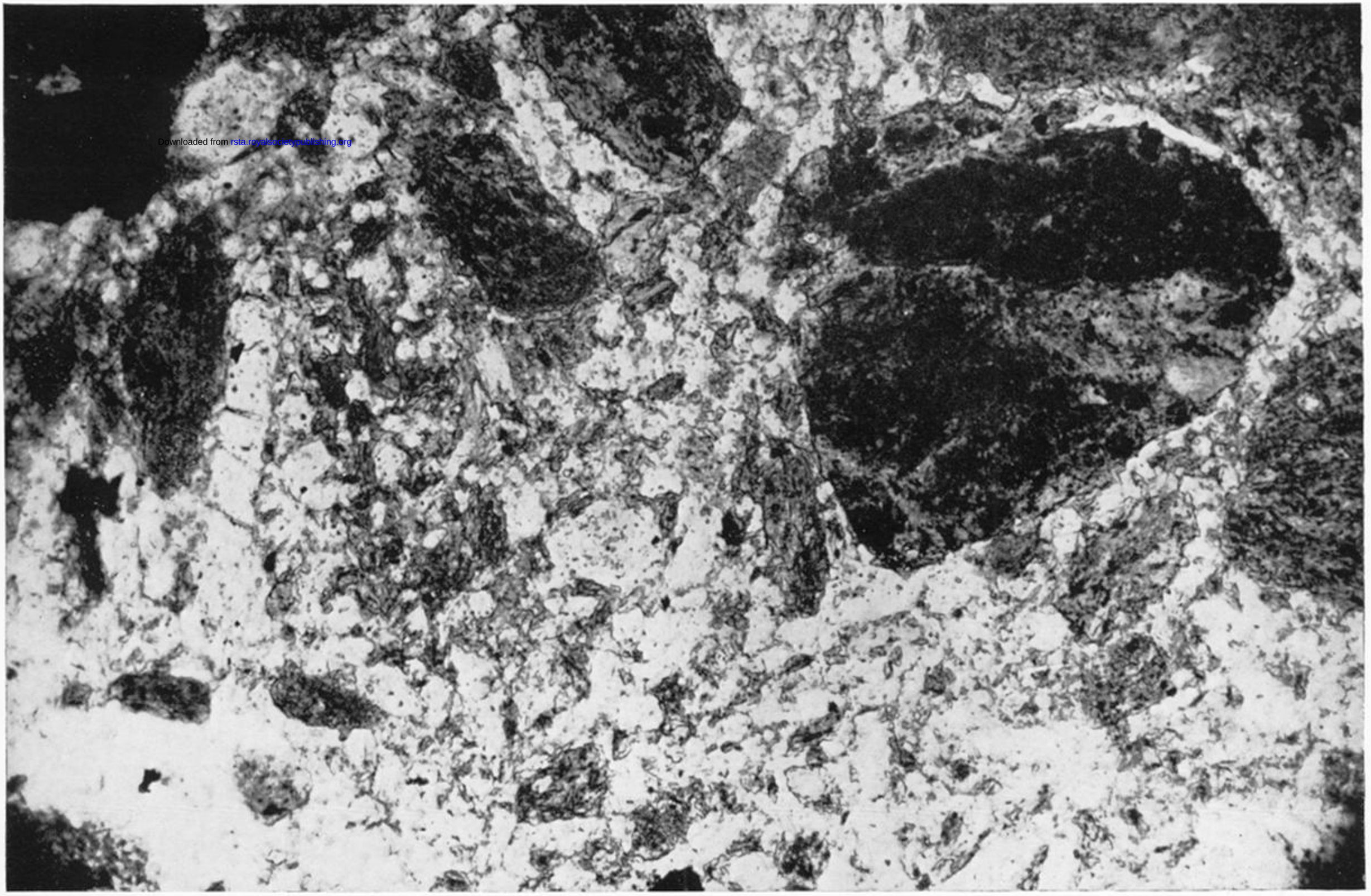

FIGURE 13. An early member of the series in which a breccia of ultramafic mineralogy is replaced by quartz. Rounded fragments of ultramafic mineralogy are set in a ground mass of rounded elongate quartz grains enclosed by flaky chlorite and talc. Ordinary light; magn. ×50.

PHILOSOPHICAL TRANSACTIONS OF THE ROYAL SOCIETY A MATHEMATICAL, PHYSICAL & ENGINEERING SCIENCES

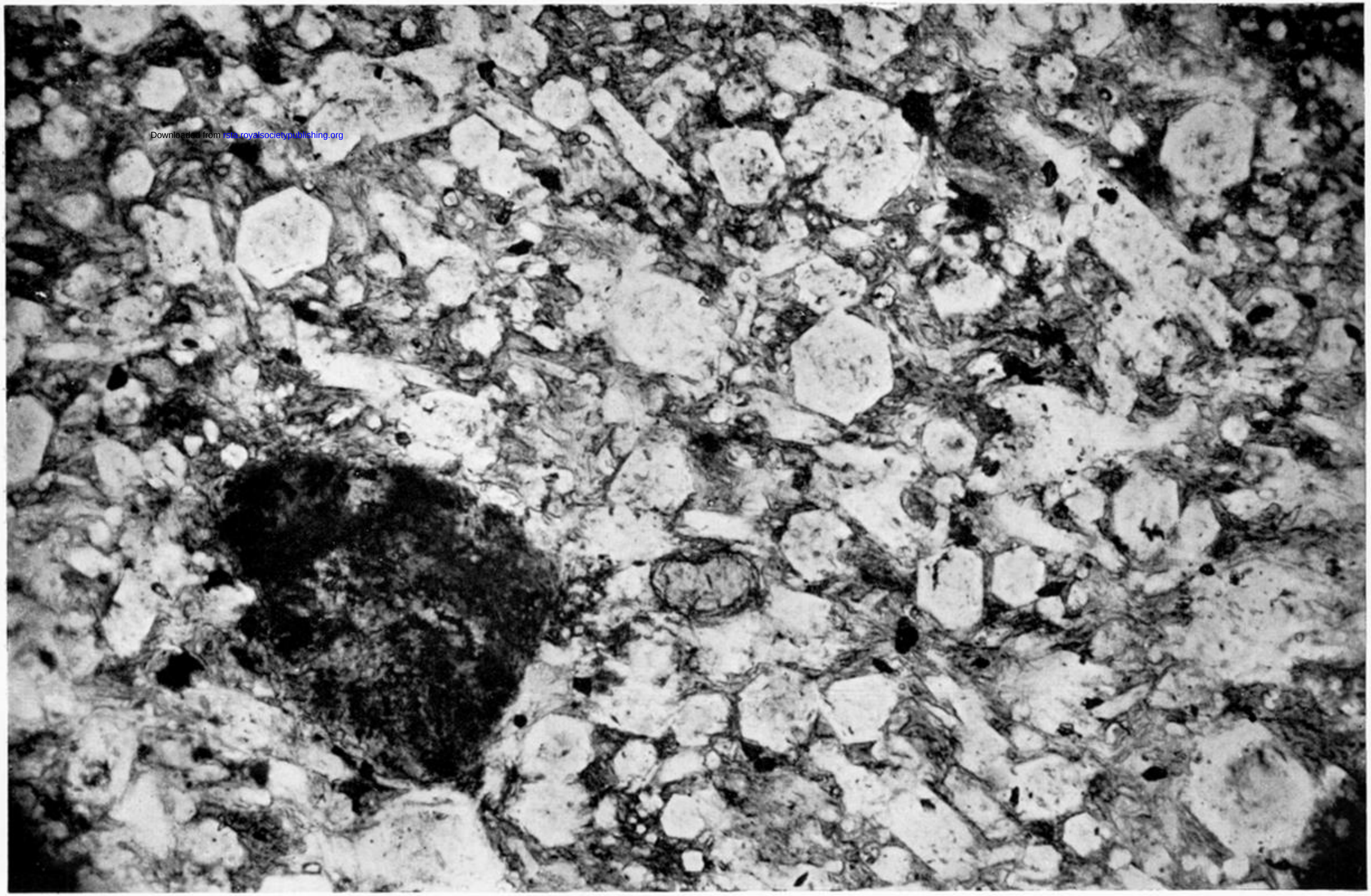

FIGURE 14. An intermediate stage in the replacement of a breccia of ultramafic mineralogy by quartz. The matrix to the ultramafic fragments is composed of euhedral quartz grains set in a base of chlorite and talc. Ordinary light; magn. $\times 50$.

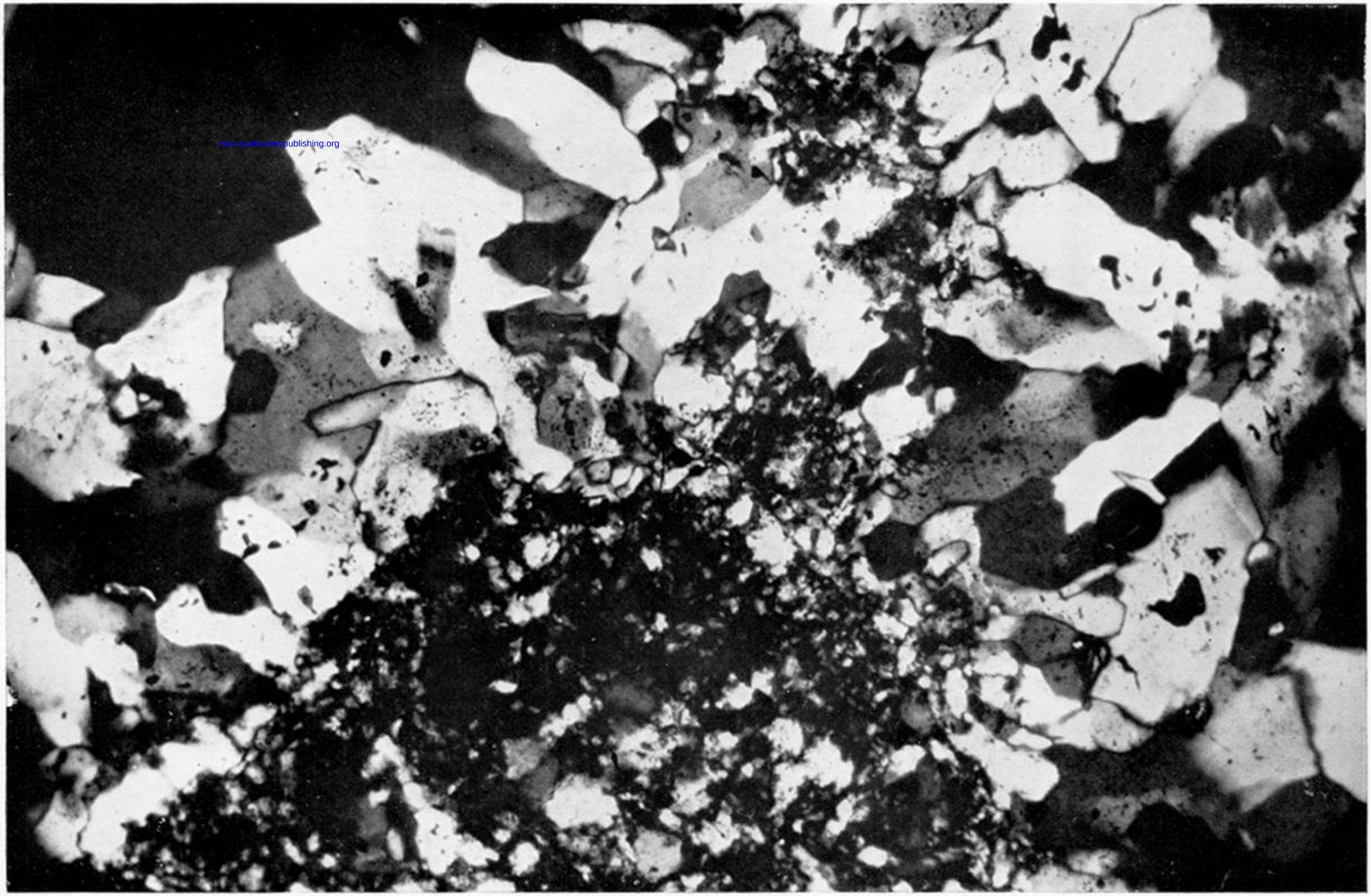

FIGURE 15. The final stage of replacement of a breccia of ultramafic mineralogy by quartz. The area of fine-grained flaky quartz represents the original breccia fragments. The matrix is composed of coarser subhedral quartz crystals. Crossed polars; magn. × 50.

PHILOSOPHICAL TRANSACTIONS OF THE ROYAL SOCIETY A MATHEMATICAL, PHYSICAL & ENGINEERING SCIENCES